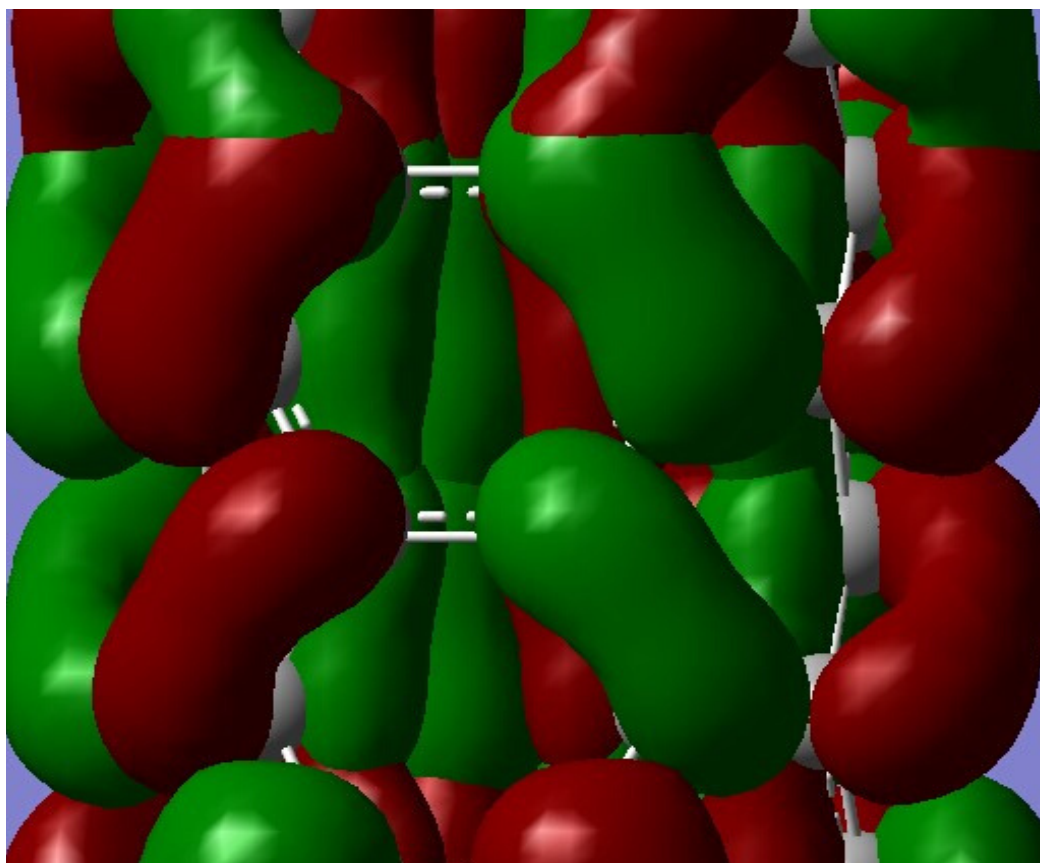


Volume 8, December 2019

ISSN 2542-2545

*The*  
**HIMALAYAN  
PHYSICS**

*A peer-reviewed Journal of Physics*



*Department of Physics, Prithvi Narayan Campus, Pokhara  
Nepal Physical Society, Western Chapter, Pokhara*

# Study on built-in potential and barrier widths of perovskite-based solar cells

Research Article

Krishna Raj Adhikari\*

Pashchimanchal Campus, Institute of Engineering, Tribhuvan University, Nepal

**Abstract:** Solar energy is the best alternative of the conventional energy sources in Nepal and as a whole in the world. The solar photovoltaic, basically based on the working principle of p-n junction diode, generates electrical energy from the solar or light energy. In this paper, the research work focuses on the built-in potential and barrier width of perovskite-based solar cells which directly affect the efficiency of the solar cells. It is observed that larger value of built-in potential and smaller value of width of depletion layer make easier to separate and transport the charge carriers to the ETM and HTM from the active layer to enhance the performance of the solar cell.

**Keywords:** Perovskite • Solar cell • Built-in potential • Barrier width • Efficiency

## 1. Introduction

Solar photovoltaic (PV) or cell, commonly made up of semiconducting materials, is a technology that directly converts solar light into electrical energy and based on the photoelectric effect. This effect was first discovered by a French Scientist Edmund Becquerel in 1839 and theorized by Einstein in 1905 [1, 2]. Working principle of most of the PV solar cells is analogous to a p-n junction diode where sole material concerned is the semiconductor [3]. Moreover, the key component of a solar cell is an absorber or active layer that absorbs the solar light to convert the light into electricity.

In 1883, Charles Fritts demonstrated a thin film selenium cell device with the efficiency around 1% and he realized enormous potential of photovoltaic devices and realized as first solar cell (Green, 1990). The next significant step forward came 49 years later, after Fritts, where the work was carried out with the copper-cuprous oxide by Grondahl over the period 1930-1932 [4] and he described the outcome of the work as the development of a rectifier and a photovoltaic cell.

It was, however, Russell Ohl, Bell laboratory Engineer, developed a “diode” in 1939 by doping one side of silicon with electron donor and other side with acceptor material. He observed an electric voltage across the

\* Corresponding Author: [adhikarikrishna@wrc.edu.np](mailto:adhikarikrishna@wrc.edu.np)

ends of the so formed “p-n junction diode” when light shone on it in 1941 who patented the modern junction semiconductor solar cell in 1946. In the same laboratory, in 1954, D. M. Chapin, C. S. Fuller, and I.G. L. Pearson developed the first “modern photovoltaic silicon cell” with the efficiency of 6% [1, 3].

The electrical performance is primarily influenced by the type of PV used where a typical module converts 6-20% of the incident solar radiation into electrical energy that depending upon the conditions of the atmosphere as well. The rest of the incident solar radiation gets converted into heat, which significantly increases the temperature of the PV module and reduces its efficiency. This heat can be extracted by flowing water/air beneath the PV module using thermal collector, called, photovoltaic thermal collectors [5].

Now, efficiency of the solar cells is above 20% and perovskite has been attracting the attention of the researchers as a solar cell material where efficiency of perovskite-based cells was already found to be exceeded 22% with hereto-junction structure. Due to different nature of materials, different types and values of dopant concentrations, surface band bending arises in the hetero-junction solar cell and hence a built-in potential develops. The minimum barrier widths of silicon-based solar cell was found to be 47 nm at 0.7 V barrier potential [6]. Usually, the barrier widths of the junctions of a solar cell directly affect the carrier transport from one region/section to the other and hence the efficiency of the solar cells.

In this research, the study has been focused on the built-in potential ( $V_{bi}$ ), barrier widths ( $W_D$ ) and performance ( $\eta$ ) of the perovskite-based hereto-junction solar cell.

## 2. Materials and Method

### Simulation

Simulation is a critical technique to realize a physical operation of the solar cell devices. Among the various simulation models, SCAPS-1D is one which is used to simulate a solar cell.

In this study, a planner hetero-junction perovskite-based solar cell was simulated. The key component i.e active layer in this solar cell is a low doped p-type methylammonium lead iodide peovskite ( $MAPbI_3$ ) with the thickness 400nm and relative permittivity 30. It is sandwiched between p-type 2, 2', 7, 7'- tetrakis- (N,N-dimethoxyphenyl-amine)-9,9'-spirobifluorene (*Spiro-MeOTAD*) of relative permittivity 3 as a Hole Transporting Material and Electron Blocked Layer (HTM) and n-type titanium oxide ( $TiO_2$ ) of permittivity 100 as the Electron Transporting Material and Hole Blocked Layer (ETM). The system with three layers was sandwiched between FTO of work function 4.4 eV and gold (Au) of work function 5.1 eV as a front and back contact respectively for effective transport and collection of electrons and holes. Simulations were carried out under 1 Sun illumination. The band tails of  $10^{14} eV^{-1}cm^{-3}$ , interface traps of  $1.0 \times 10^9 cm^{-2}$ , acceptor concentrations of  $2.14 \times 10^{17} cm^{-3}$  [3], and 300 K as working temperature were chosen in simulation to evaluate the built-in potential, thickness of depletion layer and performance of the solar cell.

The donor concentration of ETM and acceptor concentration of HTM were taken as  $5 \times 10^{19} cm^{-3}$  and

$3 \times 10^{18} \text{ cm}^{-3}$  respectively as standard values. In order to evaluate the  $V_{bi}$ ,  $W_D$  and the performance of the solar cell, donor concentration of ETM varied from  $5 \times 10^{16}$  to  $5 \times 10^{20} \text{ cm}^{-3}$ . Similarly, acceptor concentration of  $MAPbI_3$  varied from  $2.14 \times 10^{14}$  to  $2.14 \times 10^{18} \text{ cm}^{-3}$  and that is of HTM varied from  $3 \times 10^{15}$  to  $3 \times 10^{19} \text{ cm}^{-3}$ .

## Theory

The necessary underlying physics of solar cell is based on [7–9] that are discussed herein. The free charge carriers, ionized donor like and acceptor like recombination centers and some traps in a solar cell give rise to an electric field ( $E$ ) and an electrostatic potential ( $\Psi$ ) as given below:

$$\epsilon \frac{\partial^2 \Psi}{\partial x^2} = -q \left[ p - n + N_D^+ - N_A^- + \frac{\rho_{def}}{q} \right] \quad (1)$$

It is the Poisson's equation where the derivation is based on the Gauss law and  $\epsilon$  is the permittivity of the semiconductor material.

The continuity equations in terms of recombination ( $U$ ) and generation ( $G$ ) for both charge carriers are

$$-\frac{\partial J_n}{\partial x} - U_n + G = \frac{\partial n}{\partial t} \quad (\text{for electrons}) \quad (2)$$

$$\text{and } -\frac{\partial J_p}{\partial x} - U_p + G = \frac{\partial p}{\partial t} \quad (\text{for holes}) \quad (3)$$

The charge carriers are transported through the device and develop the current densities as

$$J_n = -\frac{\mu_n n}{q} \frac{\partial F_n}{\partial x} \quad (\text{for electrons}) \quad (4)$$

$$J_p = \frac{\mu_p p}{q} \frac{\partial F_p}{\partial x} \quad (\text{for holes}) \quad (5)$$

The intrinsic charge carrier in  $MAPbI_3$  perovskite was derived by using formula [10]

$$n_i = N_s \exp\left(-\frac{E_G}{2kT}\right) \quad (6)$$

where  $N_s$ ,  $E_G$ ,  $k$  and  $T$  are number of available energy states, band gap of the material, Boltzmann constant and room temperature in Kelvin respectively.

The built-in potential and barrier width/depletion layer in the hetero-junction are given by [7],

$$V_{bi} = \frac{kT}{q} \ln\left(\frac{N_A N_D}{n_i^2}\right) \quad (7)$$

$$\text{and } W_D = x_n + x_p = \sqrt{\frac{2\epsilon V_{bi} (N_A + N_D)}{q N_A N_D}} \quad (8)$$

respectively. The efficiency of the device is [7, 8],

$$\eta = \frac{FF \times J_{sc} \times V_{oc}}{P_{in}} \quad (9)$$

where  $FF$  is fill factor,  $J_{sc}$  is short circuit current,  $V_{oc}$  is open circuit voltage and  $P_{in}$  is the input solar power which is determined by the properties of the light spectrum incident upon the solar cell.

### 3. Results and Discussion

Result and Discussion The built in potential of  $TiO_2 - MAPbI_3$  and  $Spiro - MeOTAD - MAPbI_3$  depend on the intrinsic carrier concentration, dopant concentrations ( $N_D$  and  $N_A$ ) of the layer, valence/conduction band density of states and working temperature. The width of depletion layer of junction depends on the built in potential, dopant concentrations and permittivity of semiconductor materials. The used data and the result obtained after derivation and simulation are illustrated in the Table 1.

Table 1. Width of depletion layer and corresponding efficiency.

S.N.	Material	Used Data			Derived Value		$\eta$ %
		$n_i(m^{-3})$	$N_A(m^{-3})$	$N_D(m^{-3})$	$V_{bi}(V)$	$W(nm)$	
1.	$TiO_2$	$6.5 \times 10^{13}$	$2.14 \times 10^{20}$	$5 \times 10^{22}$	0.92	3796	Convergence failure
	$MAPbI_3$				0.85	3578	
	$Spiro - MeOTAD$			$3 \times 10^{21}$			
2.	$TiO_2$	$6.5 \times 10^{13}$	$2.14 \times 10^{21}$	$5 \times 10^{23}$	1.04	1276	4.68
	$MAPbI_3$				0.96	1209	
	$Spiro - MeOTAD$			$3 \times 10^{22}$			
3.	$TiO_2$	$6.5 \times 10^{13}$	$2.14 \times 10^{23}$	$5 \times 10^{25}$	1.28	141.5	22.94
	$MAPbI_3$				1.20	135.0	
	$Spiro - MeOTAD$			$3 \times 10^{24}$			
4.	$TiO_2$	$6.5 \times 10^{13}$	$2.14 \times 10^{24}$	$5 \times 10^{26}$	1.39	46.78	24.04
	$MAPbI_3$				1.32	44.74	
	$Spiro - MeOTAD$			$3 \times 10^{25}$			

The intrinsic carrier concentration of  $MAPbI_3$  were derived to be  $6.5 \times 10^{13} m^{-3}$  by using Eq. 6. Four data sets were used to calculate the built in potential, barrier width and performance of the solar cell. The third data  $N_D$  of  $TiO_2 = 5 \times 10^{25} m^{-3}$ ,  $N_A$  of  $MAPbI_3$  and  $Spiro - MeOTAD$  are  $2.14 \times 10^{23}$  and  $3 \times 10^{24} m^{-3}$  is the general and usable data set at which  $V_{bi}$ , width of depletion layer  $W_D$  and efficiency were found to be 1.28 V for  $TiO_2 - MAPbI_3$  junction and 1.20 V for  $Spiro - MeOTAD - MAPbI_3$  junction, 141.5 nm for  $TiO_2 - MAPbI_3$  junction and 135.0 nm for  $Spiro - MeOTAD - MAPbI_3$  junction and 22.94% respectively.

At  $N_D$  of  $TiO_2 = 5 \times 10^{22} m^{-3}$ ,  $N_A$  of  $MAPbI_3$  and  $Spiro - MeOTAD = 2.14 \times 10^{20}$  and  $3 \times 10^{21} m^{-3}$  respectively,  $V_{bi}$  and width of depletion layer  $W_D$  were found to be 0.92 V for  $TiO_2 - MAPbI_3$  junction and 0.85 V for  $Spiro - MeOTAD - MAPbI_3$  junction, 3796 nm for  $TiO_2 - MAPbI_3$  junction and 3578 nm for  $Spiro - MeOTAD - MAPbI_3$  junction respectively. This time efficiency is observed to be convergence failure. The low value of dopant concentrations results the low value of built-in potential and large value of the barrier widths at the both junctions. The low value of built-in potential and the large value of barrier widths make almost impossible the charge carriers to move toward the ETM and HTM from the active layer ( $MAPbI_3$ ) thence they recombine and hence the zero efficiency and convergence failure of the solar cell.

The solar cell found to be worked at  $N_D$  of  $TiO_2 = 5 \times 10^{23} m^{-3}$ ,  $N_A$  of  $MAPbI_3$  and  $Spiro-OMeTAD = 2.14 \times 10^{21}$  and  $3 \times 10^{22} m^{-3}$  respectively where the efficiency was 4.68%. Among these data, the maximum efficiency was found to be 24.04% when  $N_D$  of  $TiO_2 = 5 \times 10^{26} m^{-3}$ ,  $N_A$  of  $MAPbI_3$  and  $Spiro-MeOTAD = 2.14 \times 10^{24}$  and  $3 \times 10^{25} m^{-3}$  respectively. The built-in potential ( $V_{bi}$ ) and width of depletion layer ( $W_D$ ) were found to be 1.39 V for  $TiO_2 - MAPbI_3$  junction and 1.32 V for  $Spiro-MeOTAD - MAPbI_3$  junction, 46.78 nm for  $TiO_2 - MAPbI_3$  junction and 44.74 nm for  $Spiro-MeOTAD - MAPbI_3$  junction respectively. It has observed that larger value of dopant concentration ( $N_D$  and  $N_A$ ) resulted to the larger value of  $V_{bi}$  and smaller value of width of depletion layer. The larger value of  $V_{bi}$  and smaller value of width of depletion layer make easier to separate and transport the charge carriers to the ETM and HTM from the active layer to enhance the performance of the solar cell.

## 4. Conclusions

In this paper, study has been carried out on built-in potential, width of depletion layer and performance of the solar cell. It has been observed that the higher value of built in potential at larger dopant concentrations and smaller intrinsic carrier concentration and the working temperature. The smaller value of the barrier width is observed at the higher value of dopant concentrations and built in potential. The smaller value of width of barrier width has been made easier to separate and transport the charge carriers to the ETM and HTM from the active layer to enhance the performance of the solar cell.

## References

- [1] Green MA. Photovoltaics: coming of age. In: IEEE Conference on Photovoltaic Specialists. IEEE; 1990. p. 1–8.
- [2] Green MA. Photovoltaic principles. *Physica E: Low-dimensional Systems and Nanostructures*. 2002;14(1-2):11–17.
- [3] Adhikari KR, Gurung S, Bhattarai BK, Soucase BM. Comparative study on MAPbI<sub>3</sub> based solar cells using different electron transporting materials. *Physica Status Solidi (c)*. 2016;13(1):13–17.
- [4] Grondahl LO. The copper-cuprous-oxide rectifier and photoelectric cell. *Reviews of Modern Physics*. 1933;5(2):141–168.
- [5] Dubey S, Sarvaiya JN, Seshadri B. Temperature dependent photovoltaic (PV) efficiency and its effect on PV production in the world—a review. *Energy Procedia*. 2013;33:311–321.
- [6] Orcutt J, Ram R, Stojanović V. CMOS Photonics for High Performance Interconnects. In: *Optical Fiber Telecommunications*. Elsevier; 2013. p. 419–460.
- [7] Gray JL. The Physics of the Solar Cell. In: *Handbook of Photovoltaic Science and Engineering*. John Wiley

& Sons, Ltd; 2011. p. 82–129.

- [8] Fonash S. Solar cell device physics. 2nd ed. Elsevier; 2012.
- [9] Niemegeers A, Burgelman M, Decock K, Verschraegen J, Degraeve S. SCAPS manual. University of Gent; 2014.
- [10] Alivov Y, Singh V, Ding Y, Cerkovnik LJ, Nagpal P. Doping of wide-bandgap titanium-dioxide nanotubes: optical, electronic and magnetic properties. *Nanoscale*. 2014;6(18):10839–10849.